High performance micromachined thermopile linear arrays

Marc C. Foote and Eric W. Jones

Center for Space Microelectronics Technology
Jet Propulsion Laboratory
California Institute of Technology
Pasadena, CA 91109-8099

ABSTRACT

Linear thermopile infrared detector arrays have been produced with D* values as high as 2.2×10^9 cmHz$^{1/2}$/W for 83 ms response times. Typical responsivity is 1000 V/W. This result has been achieved with Bi-Te and Bi-Sb-Te thermoelectric materials on micromachined silicon nitride membranes. Results for several device geometries are described and compared to literature values for Schwartz type thermocouple detectors and for thin film thermopile detectors and arrays. Measurements of responsivity as a function of modulation frequency and wavelength are presented.

1. INTRODUCTION

Thermopile infrared detectors are a type of thermal detector, a class which also includes bolometers, pyroelectric and ferroelectric detectors, and Golay cells. Characteristics of thermal detectors include broadband response and, in many cases, operation without cooling. Of the various types of thermal detectors, thermopiles have the fewest requirements, making them often the simplest to incorporate into infrared systems. Thermopiles typically operate over a broad range of temperatures without cooling or temperature stabilization. Their dc response eliminates the need for a chopper. No electrical bias is required; the devices passively generate a voltage signal in response to incident radiation. If thermopiles are read out with a high impedance amplifier, they exhibit no 1/f noise.

Despite the advantages of thermopiles over other thermal detectors, they have not been developed in array formats to the extent of bolometers and ferroelectric (pyroelectric) detectors.[1,2] One difficulty in this endeavor is that the highest performance thermoelectric materials, such as Bi_2Te_3 and $Bi_{0.4}Sb_{1.6}Te_3$, are difficult to work with and are not easily incorporated into silicon fabrication lines. In addition, to achieve high system D* values, each pixel must have a separate low noise amplifier. In contrast, 2D bolometer arrays can be biased with large amplitude but short duration current pulses. In this way, bolometer pixels can be multiplexed before amplification while maintaining the device signal-to-noise ratio. Despite the difficulties in producing thermopile 2D array formats, two groups have reported significant progress towards a low cost, moderate performance, thermopile imager using modified CMOS processes.[3,4]

In this work we have produced linear thermopile arrays with significantly higher performance than previously reported for thermopile arrays. This result has been achieved with Bi-Te and Bi-Sb-Te thermoelectric materials on micromachined silicon nitride membranes. Under vacuum, room temperature D* values at zero frequency measured with a 1000 K blackbody source range from 9.7×10^8 cmHz$^{1/2}$/W to 2.2×10^9 cmHz$^{1/2}$/W for response times of 15-99 ms.

2. ARRAY DESCRIPTION

Details of the thermopile array fabrication and basic testing procedure have been described previously.[5] In brief, a silicon wafer is coated with a 600-1300 Å silicon nitride layer. Two metallization steps produce interconnect lines and pads. A photoresist lift-off stencil is patterned, then 1 μm of Bi_2Te_3 is deposited by sputtering from a compound target. A similar process is used to deposit the second thermoelectric material, which has the approximate composition $Bi_{0.55}Sb_{1.45}Te_{3.6}$. The entire structure is coated with another silicon nitride layer for passivation and mechanical support. Silicon under the devices is remove by etching in hot potassium hydroxide from the wafer backside. Slits are etched through the resulting membrane to thermally isolate individual devices. The resulting pixels are membranes connected at two ends to the silicon substrate. Each membrane consists of two silicon nitride layers, with a total thickness of about 0.6 μm, sandwiching the thermoelectric and metal lines.

Four different device geometries are discussed, represented by the photographs in Figs. 1-4. Device type 1 was designed to geometrically match a compact spectrometer.[6] Details of the test results for this type of device have been described in detail previously.[5] The other pixel designs are smaller and are more appropriate for scanned imaging applications.

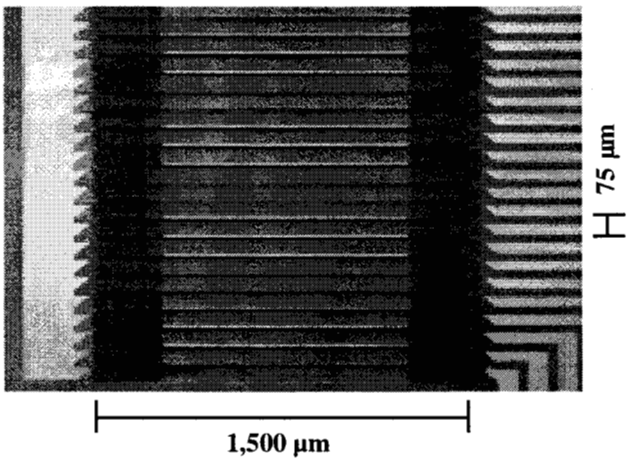

Figure 1. Array of type 1 thermopile devices. The 0.6 µm thick device membranes connect to the silicon substrate at the left and right sides. Each pixel has 11 Bi-Te / Bi-Sb-Te thermocouples in series. These long, thin devices were designed to geometrically match a spectrometer.[6]

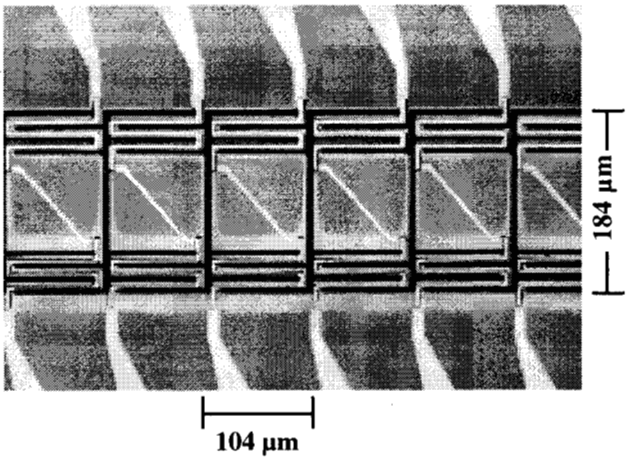

Figure 2. Array of type 2 thermopile devices. The 0.6 µm thick device membranes connect to the silicon substrate at the top and bottom. Each pixel has one Bi-Te / Bi-Sb-Te thermocouple.

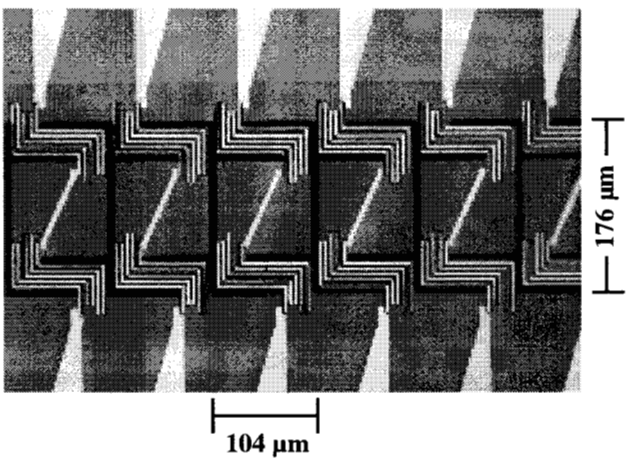

Figure 3. Array of type 3 thermopile devices. The 0.6 µm thick device membranes connect to the silicon substrate at the top and bottom. Each pixel has five Bi-Te / Bi-Sb-Te thermocouples in series.

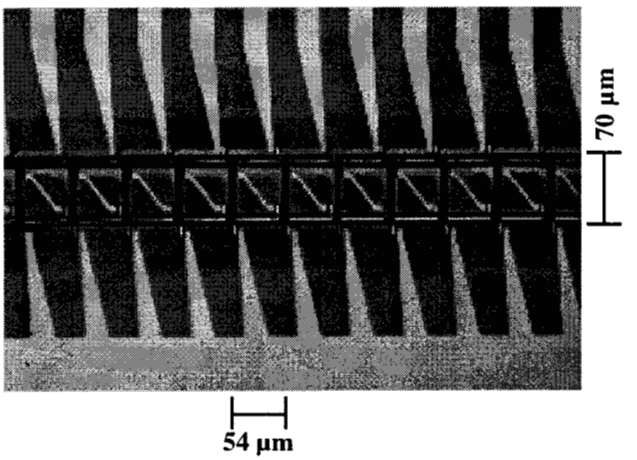

Figure 4. Array of type 4 thermopile devices. The 0.6 µm thick device membranes connect to the silicon substrate at the top and bottom. Each pixel has one Bi-Te / Bi-Sb-Te thermocouple.

3. ARRAY PERFORMANCE

Table 1 details test results on the four types of devices. Responsivity, thermal response time, and D* values are given for devices under vacuum at room temperature. The values for device type 1 represent average values of all pixels in two 63 element linear arrays. For other device types, some pixels in each array were not functional. In this case, the performance parameters are average values for functional pixels. The number of pixels used for the averages is listed. The noise in the type 1 devices was measured carefully for frequencies as low as 20 mHz, and only Johnson noise was seen.[5] For the other device types the noise was not measured, and D* was calculated with the assumption that only Johnson noise is present.

Table 1. Geometry and measured performance of the four types of thermopile devices shown in Figs. 1-4. For device types 2, 3 and 4 any non-functional pixels were ignored. The measured values represent averages of all other pixels in the arrays. The number of devices represented in the averages is listed.

PARAMETER	DEVICE TYPE 1	DEVICE TYPE 2	DEVICE TYPE 3	DEVICE TYPE 4
Detector Length (μm)	1,500	184	176	70
Pixel Pitch (μm)	75	104	104	54
Number of Thermocouples per Pixel	11	1	5	1
Number of Devices Tested	126	21	31	19
Resistance ( )	40,000	2,900	12,000	1,650
dc Infrared Responsivity (V/W)	1,100	1,120	1,060	866
Response Time (ms)	99	83	23	15
D* (1000 K, O Hz) (10^8 cmHz$^{1/2}$/W)	14	22	9.8	9.7

A comparison of the arrays produced in this work with other micromachined thermopile linear arrays is shown in Fig. 5. The data point labels indicate reference numbers. Data is not included for 2D arrays made with polysilicon thermoelectrics[3,4] due to lack of information on D* in those references. The dashed line represents the JPL results. Its slope indicates D* proportional to the square root of response time, which is typical for thermopiles or bolometers made with different geometries but using the same material system and construction.[20,21]

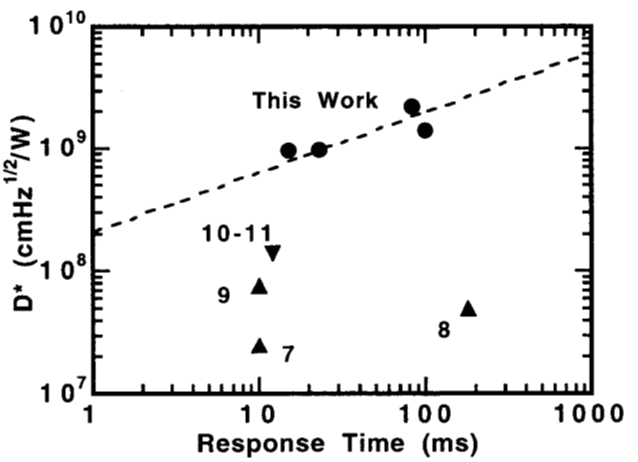

Figure 5. Representative data from the literature showing reported D* values as a function of response time for thin film thermopile linear arrays. Thermoelectric materials are Bi-Te / Bi-Sb-Te (this work) (●), constantan / chromel (▼), and silicon (▲). The dashed line represents the JPL results. Its slope indicates D* proportional to the square root of response time, which is typical for thermopiles or bolometers with different geometries and the same material system. Numbers indicate references.

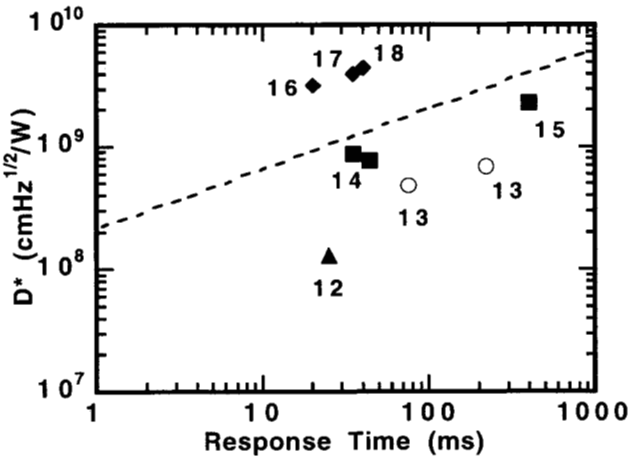

Figure 6. Representative data from the literature showing reported D* values as a function of response time for single pixel Schwartz type thermocouple detectors (◆), single pixel thin film thermopile detectors using bismuth based materials (■), single pixel thin film GaAs-AlGaAs thermopile detectors (○), and single pixel thin film silicon thermopile detectors (▲). Numbers indicate references. The dashed line represents roughly the JPL results.

Despite differences in geometry, fabrication, and testing procedures between the various arrays shown in Fig. 5, there is a clear dependence of D* on thermoelectric materials. Typically for thermocouple and thermopile detectors D* is proportional to the square root of the thermoelectric figure of merit Z,[22] defined as the square of the Seebeck coefficient divided by both the electrical resistivity and the thermal conductivity. This relationship roughly holds for devices in which a large fraction of the heat flow from the absorber occurs through the thermoelectric materials. For many thin film thermopile detectors, however, the support structure (membrane) provides a dominant part of the heat conduction path, so the dependence of D* on Z is weaker. The upright triangles in Fig. 5 indicate thermopiles made with doped crystalline silicon or polysilicon. These material systems are the most manufacturable, and should lead to the least costly commercial products. However, Z for silicon and polysilicon is relatively low (up to $4x10^{-5}$ K^{-1})[23] and the performance of devices with silicon thermoelectrics is only moderate. One should note that the D* values for silicon devices shown in Fig. 5 were measured in argon or air, while the other devices in this plot were measured in vacuum. A more favorable comparison might result if all devices were tested under vacuum. The inverted triangle, with slightly higher D*, represents arrays utilizing constantan and chromel metal film thermoelectrics, which have a somewhat higher Z value ($1x10^{-4}$ K^{-1}). The closed circles are the Bi-Te / Bi-Sb-Te devices of this work. This class of materials has Z values as high as $3x10^{-3}$ K^{-1}.

Fig. 6 shows D* versus response time for representative single pixel thermocouple and thermopile detectors reported in the literature. The dashed line roughly represents the JPL results. Again, the D* values are grouped according to materials used. The triangle is a single pixel silicon device. The open circles represent GaAs / AlGaAs, which has a thermoelectric figure of merit of about $5x10^{-5}$ K^{-1}.[13] The squares represent single pixel thin film thermopile detectors with thermocouples composed of Bi / Sb, Bi-Sb-Te / Bi-Sb, and BiSbTe+ / BiSbTe-. The performance of these bismuth-based single pixel detectors is in the same range as the JPL arrays. Significantly higher in performance are the Schwartz type thermocouples, represented by diamonds in Fig. 6. These devices are made from two pins of bulk Bi-Te or Bi-Sb-Te materials with a blackened gold foil welded across them. The performance of Schwartz thermocouples is probably the highest of any uncooled thermal detector. However, these devices are fragile, not easily arrayable, and due to their low resistance must be chopped and transformer coupled to achieve low-noise performance.

The difference in performance between the JPL arrays and the Schwartz type thermocouple detectors is predominantly due to two factors. First, the figure of merit, Z, of the bulk thermoelectric materials in Schwartz detectors is higher than that of the JPL thin films. The Schwartz thermocouple materials are grown as single crystals under optimal conditions. For example, reference 16 reports a combined Z for the two materials of 3.1 $x10^{-3}$ K^{-1}. The thermal conductivity of the JPL films was not measured, however, one can estimate Z for these films by using measured values of the Seebeck coefficient and electrical conductivity, combined with a typical Bi-Te and Bi-Sb-Te Lorenz number of $6x10^{-8}$ W/K^2 (see, for example, refs. 14 and 24). The resulting Z of roughly $1x10^{-3}$ K^{-1} for JPL films is about a factor of three lower than the best bulk materials. Thus the difference in Z accounts for a factor of square root of three in D* between the JPL arrays and the best Schwartz thermocouples.

A second reason for this difference in D* values is that the JPL detectors have significant thermal losses through the silicon nitride support structures. The thermal conductance from the absorber for JPL type 1 devices is estimated to be $1.7x10^{-7}$ W/K for the thermoelectric lines, $6.5x10^{-7}$ W/K due to radiation, and $6.7x10^{-7}$ W/K through the silicon nitride support structure. An optimized device will have no thermal link through the support structure, and equal values of thermal conductance through the thermoelectric materials and due to radiation. Theoretically, the silicon nitride could be removed from the legs of the JPL type 1 devices and the cross section of thermoelectric material could be increased to provide a thermal conductance of $6.7x10^{-7}$ W/K, matching that due to radiation. The resulting total thermal conductance would be roughly the same as its current value, so the responsivity of the devices would not change significantly. However, the device resistance would decrease by about a factor of 3.9, decreasing the noise and increasing D* by about a factor of 2.

Thus, the combination of a lower Z value and the parasitic thermal losses through the silicon nitride membrane explain the factor of 3-3.5 difference in performance between the JPL thin film arrays and the Schwartz type thermocouple detectors. To achieve the high D* of Schwartz thermocouples, the silicon nitride would have to be removed from the JPL device legs and a larger cross section of thermoelectric materials with higher Z values would be needed.

The frequency response of a type 1 device was measured as a function of chopping frequency and is shown by the data points in Fig. 7. The solid line in Fig. 7 represents $\mathcal{R} / (1+(2\pi f\tau)^2)^{1/2}$, where $\mathcal{R}$ is the measured dc responsivity, f is the chopping frequency, and τ is the measured thermal response time. The dc infrared responsivity was determined by measuring the change in device output as the shutter in front of the blackbody aperture was opened and closed. The thermal response time was measured by closing a fast shutter in front of the blackbody and monitoring the decay of the device output. This decay was exponential out to several 1/e times. The data points in Fig. 7 closely match the predicted curve.

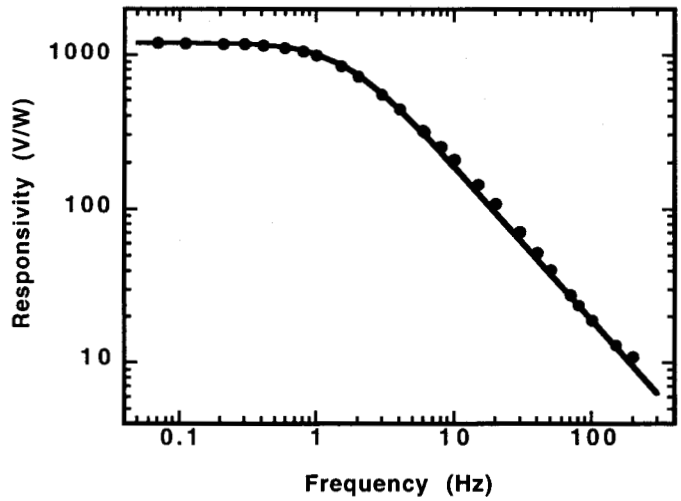

Figure 7. Data points represent measured values of responsivity versus chopping frequency for a type 1 device. The line represents $\mathcal{R}/(1+(2\pi f\tau)^2)^{1/2}$, where $\mathcal{R}$ is the measured dc responsivity, f is the chopping frequency, and τ is the measured thermal response time.

Fig. 8 shows the spectral response for two type 1 detectors from different wafers. The radiation from a glow bar passed through a grating monochromator; unwanted diffraction orders were eliminated with a high pass filter. The monochromatic beam was split, with part going to the detector under test and part to a blackened pyroelectric detector. To increase the thermopile detector absorption, a thin layer of platinum with resistance approximately 200 /square was deposited on the backside of the membranes. Both thermopile detectors shown in Fig. 8 have fairly flat broadband response. The difference in wavelength dependence is probably due to silicon nitride and platinum thickness differences between the two wafers.

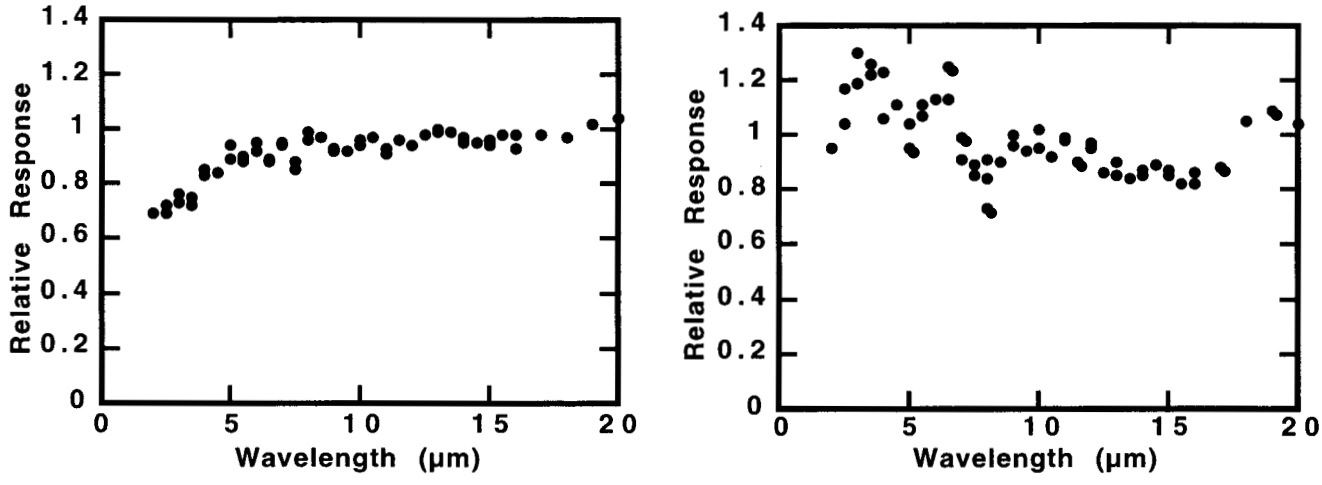

Figure 8. Relative spectral response curves for JPL type 1 devices from two different wafers. Differences in spectral response are probably due to different silicon nitride and platinum thicknesses. The curves demonstrate the broadband nature of these devices.

4. SUMMARY

Linear thermopile infrared detector arrays, using Bi-Te and Bi-Sb-Te thermoelectric materials on micromachined silicon nitride membranes, have been produced with D* values as high as 2.2×10^9 cmHz$^{1/2}$/W for 83 ms response times. Typical responsivity is 1000 V/W. Spectral response is fairly flat, and the frequency variation of responsivity is consistent with the measured values of dc responsivity and response time. Obtaining the high D* of Schwartz thermocouples would require removal of the silicon nitride in the device legs and a larger cross section of thermoelectric materials with higher Z.

5. ACKNOWLEDGMENTS

The authors are grateful to Thierry Caillat for assistance in fabricating the sputter targets and for helpful discussion. Professor Tom Kenny of the Mechanical Engineering Department of Stanford University supplied the CVD silicon nitride films. The research described in this paper was performed by the Center for Space Microelectronics Technology, Jet Propulsion Laboratory, California Institute of Technology, and was sponsored by the National Aeronautics and Space Administration, Office of Space Science.

6. REFERENCES

1. R.A. Wood, "Uncooled thermal imaging with monolithic silicon focal planes", *Proc. SPIE 2020, Infrared Technology XIX*, pp. 322-329, 1993.
2. Charles Hanson, "Uncooled thermal imaging at Texas Instruments", *Proc. SPIE 2020, Infrared Technology XIX*, pp. 329-336, 1993.
3. T. Kanno, M. Saga, S. Matsumoto, M. Uchida, N. Tsukamoto, A. Tanaka, S. Itoh, A. Nakazato, T. Endoh, S. Tohyama, Y. Yamamoto, S. Murashima, N. Fujimoto, and N. Teranishi, "Uncooled infrared focal plane array having 128x128 thermopile detector elements", *Proc. SPIE Vol. 2269, Infrared Technology XX*, pp. 450-459, 1994.
4. A.D. Oliver, W.G. Baer, and K.D. Wise, "A Bulk-Micromachined 1024-Element Uncooled Infrared Imager", *Proc.of the 8th Int. conference on Solid-State Sensors and Actuators (Transducers '95), and Eurosensors IX*, pp. 636-639, 1995.
5. M.C. Foote, E.W. Jones and T. Caillat, "Uncooled Thermopile Infrared Detector Linear Arrays with Detectivity Greater than 10^9 $cmHz^{1/2}/W$", accepted for publication in *IEEE Transactions on Electron Devices*, 1998.
6. Edward Johnson, Andrew Bodkin and Michael Groden, Ion Optics, Inc., Waltham, MA.
7. I.H. Choi and D.D. Wise, "A Silicon-Thermopile-Based Infrared Sensing Array for Use in Automated Manufacturing", *IEEE Transactions on Electron Devices*, vol. ED-33, pp. 72-79, 1986.
8. P.M. Sarro, H. Yashiro, A.W. v. Herwaarden and S. Middelhoek, "An Integrated Thermal Infrared Sensing Array", *Sensors and Actuators*, vol. 14, pp. 191-201, 1988.
9. Wayne G. Baer, Khalil Najafi, Kensall D. Wise and Robert S. Toth, "A 32-element micromachined thermal imager with on-chip multiplexing", *Sensors and Actuators A*, vol. 48, pp. 47-54, 1995.
10. R.A. Wood, T.M. Rezachek, P.W. Kruse and R.N. Schmidt, "IR SnapShot Camera", *Proc. SPIE 2552, Infrared Technology XXI*, pp. 654-660, 1995.
11. A. Wood, private communication.
12. M. Müller, W. Budde, R. Gottfried-Gottfried, A. Hübel, R. Jähne and H. Kück, "A Thermoelectric Infrared Radiation Sensor With Monolithically Integrated Amplifier Stage and Temperature Sensor", *Proceedings of the 8th International Conference on Solid-State Sensors and Actuators (Transducers '95), and Eurosensors IX*, pp. 640-643, 1995.
13. A. Dehé and H.L. Hartnagel, "Free-Standing AlGaAs Thermopiles for Improved Infrared Sensor Design", *IEEE Transactions on Electron Devices*, vol. 43, pp. 1193-1199, 1996.
14. F. Volklein, A. Wiegand and V. Baier, "High-sensitivity radiation thermopiles made of Bi-Sb-Te films", *Sensors and Actuators A*, vol. 29, pp. 87-91, 1991.
15. V.V. Razinkov, N.K. Tsypdo, V.V. Gritsai, "High-Responsive Thermoelectric Radiation Receivers", *Journal of Thermoelectricity*, vol. 1 no. 1, pp. 62-66, 1993.
16. E. Ando, "Radiation Thermocouples with $(Bi,Sb)_2(Te,Se)_3$", *Japanese Journal of Applied Physics*, vol. 13, pp. 863-869, 1974.
17. R. Fettig, M. Balzer, U. Birdholz, J. Hofman and H. Meyer, "Thermoelectric IR-Detectors", *Proceedings of the Eighth International Conference on Thermoelectric Energy Conversion and the Second European Conference on Thermoelectrics*, pp. 220-223,1989.
18. O.I. Kupchinskii, P.A. Bogomolov, I.P. Zabolotskii, *Opt. Mekh. Prom.*, No. 8, p. 27, 1961. This work is summarized in English in reference 19.
19. N.A. Pankratov, "Modern semiconductor thermoelectric radiation detectors", *Sov. J. Opt. Technol.*, vol. 60, pp. 522-529, 1993.
20. R. C. Jones, "Factors of Merit for Radiation Detectors", *Journal of the Optical Society of America*, vol. 39, pp. 344-356, May 1949.
21. R. C. Jones, "A New Classification System for Radiation Detectors", *Journal of the Optical Society of America*, vol. 39, pp. 327-343, May 1949.
22. D. F. Hornig and B. J. O'Keefe, "The Design of Fast Thermopiles and the Ultimate Sensitivity of Thermal Detectors", *The Review of Scientific Instruments*, vol. 18, pp. 474-482, July 1947.
23. R. Lenggenhagger, H. Baltes and T. Elbel, "Thermoelectric infrared sensors in CMOS technology", *Sensors and Actuators A*, vol. 37-38, pp. 216-220, 1993.
24. H. Scherrer and S. Scherrer, "An Overview of the Thermoelectric Properties of the Ternary (Bi,Sb,Te) and (Bi,Te,Se) Systems", *Proceedings of the 12th International Conference on Thermoelectrics*, pp. 90-96, 1993.